Apoptosis (2006) 11:2147–2157
DOI 10.1007/s10495-006-0197-3

Uev1A, a ubiquitin conjugating enzyme variant, inhibits stress-induced apoptosis through NF-κB activation

Noor A. Syed · Parker L. Andersen · Robert C. Warrington · Wei Xiao

Published online: 12 October 2006

Abstract We have previously shown that *UEV1* is up-regulated in all tumor cell lines examined and when SV40-transformed human embryonic kidney cells undergo immortalization; however, it is unclear whether and how *UEV1* plays a critical role in this process. *UEV1A* encodes a ubiquitin conjugating enzyme variant, which is required for Ubc13 (ubiquitin conjugating enzyme) catalyzed poly-ubiquitination of target proteins through Lys63-linked chains. One of the target proteins is NEMO/IKKγ (nuclear factor-κB essential modulator/inhibitor of κB protein kinase), a regulatory subunit of IκB kinase in the NF-κB signaling pathway. In this report, we show that constitutive high-level expression of *UEV1A* alone in cultured human cells was sufficient to cause a significant increase in NF-κB activity as well as the expression of its target anti-apoptotic protein, Bcl-2 (B-cell leukemia/lymphoma 2). Overexpression of *UEV1A* also conferred prolonged cell survival under serum-deprived conditions, and protected cells against apoptosis induced by diverse stressing agents. All of the effects of Uev1A were reversible upon suppression of *UEV1* expression by RNA interference. Our observations presented in this report provide evidence that Uev1A is a critical regulatory component in the NF-κB signaling pathway in response to environmental stresses and identify *UEV1A* as a potential proto-oncogene.

N. A. Syed · P. L. Andersen · W. Xiao (✉)
Department of Microbiology and Immunology, University of Saskatchewan, Saskatoon, Saskatchewan, S7N-5E5, Canada
e-mail: wei.xiao@usask.ca

R. C. Warrington
Department of Biochemistry, University of Saskatchewan, Saskatoon, Saskatchewan S7N 5E5, Canada

Keywords Uev1A-Ubc13 · Lys-63 poly-ubiquitination · NF-κB · Cancer · Apoptosis

Introduction

UEV1 (also known as *CROC1* or *CIR1*) encodes an ubiquitin (Ub) conjugating enzyme (Ubc) variant (Uev). It was initially reported as a transactivator of the *c-fos* promoter [1]. *UEV1* was independently isolated by two mRNA differential display screens, and was found to be down-regulated in HT-29-M cells undergoing differentiation [2], and up-regulated when SV40-transformed human embryonic kidney cells become immortal [3]. *UEV1* was also identified as a putative homolog of the yeast *MMS2* involved in DNA postreplication repair [4], and found to be variously up-regulated in all tumor cell lines examined [5]. *UEV1* maps to chromosome 20q13.2 [2], a region where DNA amplification is frequently reported in breast cancers [6–9] and other tumors [10], as well as in virus-transformed immortal cells [11] and those overcoming cellular senescence in cancer pathogenesis [12]. These observations collectively establish a close correlation between *UEV1* expression and tumorigenic potential; however, whether *UEV1* plays a role in promoting tumorigenesis and how this is accomplished remains to be elucidated.

Uev1 is a member of the protein family that serves as a co-factor for Ubc13-catalyzed Lys63-linked poly-Ub chains [13–16]. Post-translational modification of proteins via Lys48-linked poly-Ub has been well characterized as a signal for protein degradation by the 26S proteosome, but relatively less is known about the covalent modification of proteins via Lys63 poly-Ub chains which regulate diverse functions in a non-proteolytic manner [17]. So far, Ubc13 is the only known Ubc capable of mediating Lys63-linked poly-Ub chains, and this process requires a Uev. Uev has an

amino acid sequence similar to that of an Ubc, but lacks an essential Cys residue in the proposed active site. Although this renders Uev catalytically inactive [2, 4, 5], it can interact physically with Ubc13 to mediate Lys63 poly-Ub chain assembly [13, 16].

Recent reports indicate that the Uev-Ubc13 heterodimer is involved in TRAF6-[tumor-necrosis factor (TNF) receptor-associated factor 6] [18, 19] and TRAF2-mediated [20] activation of NF-κB. Under normal conditions, activation of the NF-κB signal transduction pathway is initiated by extracellular signals such as TNF, interleukins, UV irradiation, and bacterial or viral infections. Upon stimulation, membrane-associated protein complexes activate single or multiple cascades of events that eventually converge onto IKK (inhibitor of κB protein kinase), which consists of two kinase subunits (IKKα and IKKβ) and a regulatory subunit known as IKKγ or NEMO (NF-κB essential modulator). These events culminate in phosphorylation of IκBα, an inhibitory protein that retains NF-κB Rel (p65) subunits in the cytoplasm. Phosphorylated IκBα is selectively ubiquitinated and degraded, freeing the Rel family of transcriptional activators to translocate into the nucleus and activate an array of target genes [21, 22]. The role of Lys63 poly-Ub modifications in the NF-κB cascade has recently received great attention. We and others [23, 24] have shown that NEMO is a cellular target of Lys63 poly-Ub, which requires the Ubc13-Uev1 complex with TRAF2, TRAF6 or paracaspase as a Ub ligase. The Ubc13-Uev1 heterodimer is also involved in Lys63 poly-Ub of RIP1, which is required for NF-κB activation in response to TNFα [25].

NF-κB activation is considered to be a pro-survival and anti-apoptotic response, constitutive activation of NF-κB has been linked to many types of cancers [21, 26]. One of the downstream target genes transcribed by NF-κB is the anti-apoptotic human *Bcl-2* gene [27, 28]. The Bcl-2 oncoprotein is frequently overexpressed in colon cancers [28–30]. In addition activation of NF-κB is linked to inflammatory and immune response and very recently it has been reported that chronic NF-κB activation is essential for inflammation-associated progression of cancer [31–34]. Based on the above observations, we hypothesized that overexpression of *UEV1A* alone may be sufficient to drive cells toward tumorigenesis. Our findings presented in this report are consistent with *UEV1A* as an anti-apoptotic and pro-inflammatory factor involved in the NF-κB pathway.

Materials and methods

Cell culture

Delbecco's modified essential medium (DMEM) was purchased from Sigma (Oakville, Ontario, Canada) and horse serum and trypsin/EDTA were from Invitrogen (Burlington, Ontario, Canada). HepG2 and HeLa cells were maintained in DMEM supplemented with 10% horse serum in a humid incubator at 37°C with 5% CO_2.

Plasmids and transfection

Constructs to express Myc-tagged Uev1 were made as follows. The entire open reading frame of *UEV1A* without the stop codon was PCR-amplified as a *Bam*HI-*Xho*I fragment and cloned into the same sites of pcDNA3.1/Myc-His(+)A (Invitrogen). The *UEV1A* gene expression was under the transcriptional control of a cytomegalovirus (CMV) constitutive promoter and fused with the Myc-His_6 coding region at the C-terminus.

Transfections were done on ~80–90% confluent serum-starved cells in 100 mm cell culture dishes. Stable cell lines were created by transfecting HepG2 or HeLa cells with 12 μg of circular plasmid DNA (pcDNA-Uev1A or pcDNA3.1) using Lipofectamine-Plus reagent from Invitrogen. After three hours, 10% horse serum was added and the cells were incubated overnight. On the next day transfection media were changed to fresh media containing 10% horse serum and cells were grown one more day. On the third day the cells were passaged into new medium with 2 mg/mL Geneticin (G418, Invitrogen). The selection pressure was maintained for 20 days and approximately 70 G418-resistant colonies were picked and grown in 96-well tissue culture dishes. The screening process for Uev1A-Myc positive clones was done by Western blot analysis using mouse anti-c-Myc monoclonal antibody from Oncogene (San Diego, USA) or Sigma. HepG2 clones C1 and C2 were selected to represent high-level Uev1-Myc expressing cell lines and C6 was selected to represent low-level Uev1-Myc expressing cell lines. In all experiments tested, C1 and C2 behaved indistinguishably, while C6 phenotypes are very similar to those of vector-transfected (control) cells. Hence, only C1 and control cells are shown in this report.

Two approaches were taken to silencing target *UEV1* expression. Initially, the RNA interference construct against *UEV1* was made by cloning double stranded oligonucleotides at the *Xba*I and *Bbs*I sites of mU6pro plasmid as described [35], with the target sequence 5′-GACATGACACTTACAAGATGG-3′. The transfection method was as above except that 4 μg of plasmid DNA was used and transfected cells were passaged and grown in medium supplemented with 10% horse serum for seven days before assessing Uev1A-Myc levels by Western blot analysis using anti-c-Myc antibody. It has been previously established by immunocytochemistry that with a standard protocol, expression of the target protein was reduced in approximately 90% of cells and that a single nucleotide mismatch in the RNAi sequence abolished the suppression

[36]. Subsequently, Qiagen designed HP Validated siRNA and nonsilencing control siRNA (Qiagen Inc., Mississauga, Ontario, Canada) were transfected into C1 and C2 cells. The reduction of *UEV1A* was confirmed by Western blot analysis and further by real-time RT-PCR. RNA was isolated using RNA isolation kit by Qiagen and cDNA synthesized by ThermoScript™ RT-PCR system from Invitrogen. Real-time PCR was performed on a MiniOpticon machine from Bio-Rad, with QuantiTech Primer Assay from Qiagen using iTaq SYBR green supermix (Bio-Rad). All procedures were followed as described by the manufactures protocols.

Western blot analysis

Confluent (80–90%) transfected cells grown in 100 mm plates were washed twice with ice-cold PBS (phosphate-buffered saline, containing 140 mM NaCl, 2.7 mM KCl, 10 mM Na_2HPO_4, 1.8 mM KH_2PO_4, pH 7.4) and lysed using 0.5 mL of lysis buffer containing 50 mM HEPES (pH 7.4), 150 mM sucrose, 2 mM sodium orthovanadate, 80 mM β-glycerophosphate, 10 mM sodium fluoride, 10 mM sodium tetrapyrophosphate, 2 mM Na-EGTA, 2 mM Na-EDTA, 1% Triton X-100, 0.1% SDS, 1 mM phenyl methyl sulphonyl fluoride, 10 μg/mL aprotinin, 10 μg/mL leupeptin and 10 μg/mL trypsin inhibitor (Sigma). Plates were kept on ice for 30 min and then scraped and lysates were kept at -70°C. Before using, samples were thawed on ice and centrifuged at 13,000 *g* for 2 min at 4°C, and the resulting supernatants were used for experiments. Protein concentration was determined on the supernatants using Bradford protein assay reagents from Bio-Rad. SDS-PAGE sample buffer was mixed with 20–25 μg of protein sample, boiled for 5 min and proteins separated by electrophoresis through 12% SDS-PAGE. Resolved proteins were transferred onto PVDF membrane (Perkin Elmer Life Sciences Inc., Boston, USA). The membranes were blocked with 5% blotting skim milk (Bio-Rad) in 0.02% Tween 20/PBS for 3 hr prior to incubating overnight at 4°C with primary antibodies, including mouse anti-c-Myc (1:1000), mouse anti-Bcl-2 (1:1000), mouse anti-β-actin (1:3000) from Sigma, or mouse anti-p$I\kappa B\alpha$ (1:1000) from Cell Signaling (Danvers, MA, USA). On the next day the membranes were washed and incubated with horseradish peroxidase-conjugated anti-mouse secondary antibody (1:10,000) from Upstate (UBI, Lake Placid, NY, USA) for one hr at room temperature. The membranes were washed and protein bands were visualized with the aid of the Western lightning chemiluminescence detection system from Perkin Elmer.

NF-κB luciferase reporter assay

Stably transformed HepG2 or HeLa cells were transiently transfected with 1.0 μg pLam3 (NF-κB responsive luciferase) and 0.01 μg pR-TK (Renilla luciferase control vector) (both of these constructs were generously provided by Dr. V.M. Dixit, Genentech Inc., San Francisco, USA). Transfection method used was as described above and NF-κB reporter activity was measured 24 hr post-transfection using the Dual Luciferase Reporter Assay System (Promega, Madison, WI, USA) by following the supplier's protocol.

Immunocytochemistry

Stably transfected HepG2 cells grown on 18 mm round glass cover slips (VWR) were treated as described in figure legends. The cells were then fixed in 3.7% formaldehyde for 30-min at room temperature. After rinsing 4 times over a 30 min period in PBS, cells were permeabilized in 0.5% Triton X-100/PBS for 5 min at room temperature. This was followed by a rinse in PBS and then blocking in 2% skim milk/PBS for 1 hr at room temperature. To each cover slip was added 100 μL of rabbit anti-p65 antibody from Santa Cruz Biotechnology (diluted 1:100 in blocking solution). After 30 min incubation, the cover slips were washed 4 times over a 30-min period with PBS and incubated with Alexa 546 from Molecular Probes (Eugene, OR, USA) secondary antibody (diluted 1:2000 in blocking solution). Finally cover slips were mounted onto glass slides with CitiFluor™ mounting media from Marivac (Montreal, Canada). The mounting media contained 2 μg/mL DAPI (4′,6-Diamidino-2-phenylindole) (Sigma) to locate the nuclei. Translocation of p65 was visualized under an Olympus 1X70 inverted fluorescence microscope with appropriate filter and digital images captured by "Spot Advance" software with an RT slider camera.

Flow cytometry and TUNEL analysis

Flow cytometry analysis was performed essentially as previously described [37] with modifications. Approximately 1×10^6 cells were plated in 100 mm dishes, treated with or without 0.1 μM CPT (Camptothecin, from Sigma) for 48 hr or 1.0 μM STS (Staurosporine, from Sigma) for 24 hr. Cells were trypsinized, collected and washed in ice-cold PBS and fixed in 1.0 mL of 70% ethanol. The samples were stored at -20°C until use. At the time of analysis the samples were centrifuged and the pellets were suspended in 1 mL of PBS containing 1 mg/mL RNase and 50 μg/mL propidium iodide (Sigma), incubated at 37°C for 30 min in the dark, and analyzed by flow cytometry using an EPICS XL flow cytometer (Coulter Electronics, Miami, USA). At least 20,000 events were acquired for each sample.

Assessment of apoptotic nuclei was also performed by a (TdT)-mediated dUTP nick end-labeling (TUNEL) assay using the DeadEnd™ Fluorometric TUNEL system purchased from Promega. TUNEL analysis was performed on stable cells grown on 18 mm round glass cover slips. Nuclei were

visualized by DAPI staining under an Olympus 1X70 inverted fluorescence microscope under the appropriate filter. Digital images were captured using the "Spot Advance" software with a RT Slider camera.

Cell count

Transfected HepG2 cells were equally seeded into 60 mm tissue culture dishes with or without 10% horse serum. Each consecutive day cells were fixed by addition of 3.7% formaldehyde directly to the medium and left at 4°C for at least 30 min. This was followed by a wash with PBS and the addition of 2 μg/mL DAPI in PBS. DAPI-stained intact nuclei were counted as number per field of view under an Olympus 1X70 inverted fluorescence microscope.

Soft agar assay

Anchorage-independent growth ability of stably transfected HepG2 cells was determined by the method as described [38] with modifications. Briefly 1×10^3 cells/mL were mixed with 0.4% Bacto Agar Select (BD Biosciences, San Jose, CA, USA) in DMEM media with 20% horse serum and layered onto five 100 mm tissue culture dishes pre-coated with 0.6% Bacto Agar Select in DMEM/20% horse serum. The plates were transferred to a 37°C incubator with 5% CO_2. Colonies were counted at day 5, 10, 15, 20 and 25 as number per field of view under a microscope at 20X objective. Furthermore on day 25, plates were stained with 0.1% crystal violet dye and visible colonies were also counted.

Results

Constitutive overexpression of *UEV1A* results in NF-κB activation and increased Bcl-2 protein

Human *MMS2* and *UEV1* are two *UEV* genes that have been shown [5] to share >90% amino acid sequence identity in their core domains. We have previously determined that *hMMS2* is involved in DNA repair like its yeast counterpart [39], whereas inhibition of *UEV1* does not compromise DNA repair activities [36]. Hence, we hypothesize that only *UEV1* is involved in the NF-κB signaling pathway. *UEV1* encodes two alternative splicing products, Uev1A and Uev1B with an identical core Uev domain but different N-termini [1, 5]. However, only Uev1A is capable of interacting with Ubc13 and inhibition of *UEV1* specifically affects NF-κB activation [36]. In order to determine the biological effects of *UEV1A* overexpression, we fused the *UEV1A* open reading frame with Myc-His_6 under the control of a constitutive CMV promoter and established stable HepG2 cells expressing variable levels of Uev1A-Myc as judged by Western blot analysis using an anti-Myc antibody (Fig. 1(A)). For subsequent experiments we chose to use C1, C2 (high-level expression) and C6 (expressing 10% of Uev1A-Myc compared to C1 or C2) clones to assess effects of *UEV1A* expression on cellular functions. Presently, we are restricted to using antibody detection of the Myc-tagged protein because there is no specific antibody to detect endogenous Uev1A alone in cells. Polyclonal and monoclonal antibodies raised against hMms2 in our laboratory were unable to specifically differentiate between endogenous Uev1A and hMms2 by Western blot analysis; mass spectrophotometry analysis confirmed that endogenous hMms2 and Uev1A comigrate during electrophoresis (data not shown). In order to reverse the *UEV1A*-overexpressed phenotype, we achieved significant

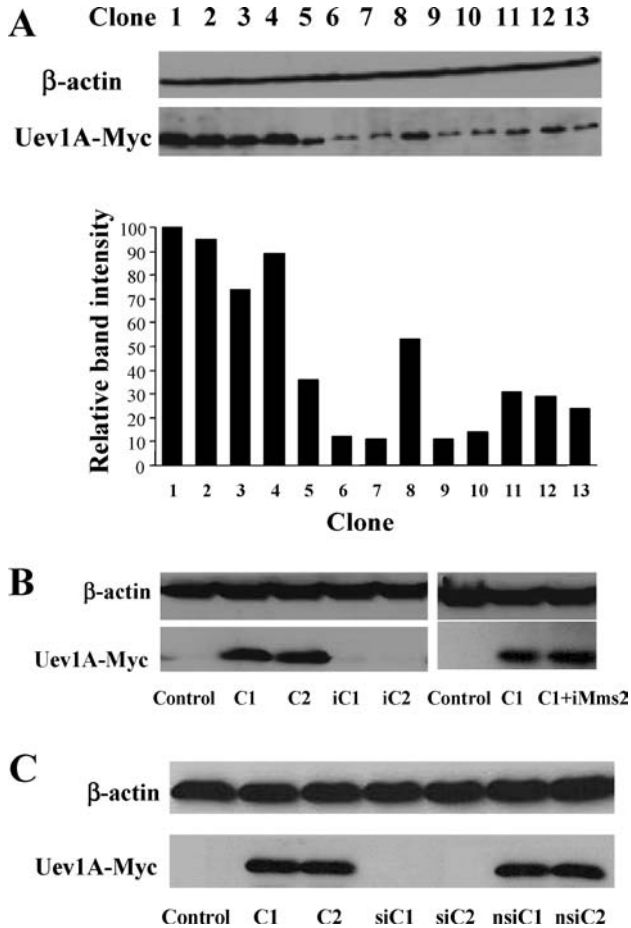

Fig. 1 Establishment of HepG2 cell lines overexpressing Uev1A-Myc. (A) Western blot analysis of Uev1A-Myc expression in selected G418-resistant clones and assessment of their relative levels of Uev1A-Myc, using C1 cell line as a reference. (B) Western blot analysis of vector-transfected (control), C1 and C2 cells, and C1 and C2 cells transfected with RNAi construct against *UEV1* expression (iC1 and iC2). RNAi against Mms2 is shown here as a nonsilencing control. (C) Silencing of Uev1A-Myc using Qiagen HP validated shiRNA against *UEV1* in C1 (siC1) and C2 (siC2) cells, and nonsilencing control shiRNA (nsiC1 and nsiC2). 20 μg of cell lysates from various cell lines were loaded and the Uev1-Myc level was monitored by Western blot analysis with an anti-Myc antibody (bottom panel). Equal loading was monitored by β-actin detection (top panel)

abrogation of Uev1A-Myc by using RNA interference (RNAi) technology [35] against *UEV1* that we designed in our lab (Fig. 1(B)) and also used HP validated siRNA designed by Qiagen (Fig. 1(C)). The RNAi suppression effect on the target *UEV1* was highly specific as judged by our control experiments with scrambled RNAi in our previous publication [36] and shown here by RNAi against Mms2 (iMms2, Fig. 1(B)) and by using a nonsilencing (nsi) control purchased from Qiagen (Fig. 1(C)). It was determined by a real-time PCR method that, compared with untransfected or vector-transfected cells, the *UEV1A* transcript level in C1 cells is about 2.5 fold while siRNA against *UEV1* treatment reduced its transcript level to 0.15 fold (data not shown), which is consistent with Western blot analyses.

One of our major aims was to determine whether *UEV1A* overexpression results in NF-κB activation; therefore, we compared NF-κB activity in control and *UEV1A*-overexpression cell lines. The NF-κB activity was determined by NF-κB-responsive luciferase reporter assay, by IκBα phosphorylation and by p65 (RelA) translocation into the nucleus. Using the Dual Luciferase Assay system, we found that overexpression of Uev1A-Myc alone in HepG2 cells was sufficient to cause up to 10-fold increase in NF-κB activity as compared to control cells (Fig. 2(A)). Consistent with this, phosphorylated species of IκBα was also detected in *UEV1A* overexpressing cells but not in control transfected cells, which was accompanied with a decrease in total IκBα protein in C1 cells as compared to control and iC1 (Fig. 2(B)). Consequently we found that *UEV1A* overexpression also resulted in spontaneous nuclear localization of Rel/p65 in approximately 43% of the cells without any external stimulation, whereas none of the control cells displayed p65 nuclear localization (Figs. 2(C) and (D)). Furthermore, to ask whether the increased NF-κB activity seen in C1 cells resulted in downstream signaling events, we analyzed the expression of a representative NF-κB target gene. The level of Bcl-2, a well known anti-apoptotic protein induced by NF-κB activation [29, 40, 41], indeed increased significantly in C1 cells as compared to control (Fig. 2(E)). This effect of *UEV1A* overexpression was reversed by RNAi against *UEV1A* (siC1). We had to load more total protein to detect endogenous Bcl-2 because in HepG2 cells endogenous Bcl-2 expression was reported to be very minute or not detectable [42–44]. In light of these previous reports, our results were very significant and demonstrate that this up-regulation of Bcl-2 is indeed due to overexpression of *UEV1A* in HepG2 cells.

Several lines of evidence support our argument that the observed NF-κB activation is specifically due to *UEV1A* overexpression. First, the p65 nuclear localization was correlated with the level of heterologous *UEV1A* expression. For example, cell line C6 expressed a low level of *UEV1A* and did not display an apparent increase in p65 nuclear localization, whereas other independent high-level *UEV1A* expression cell lines (C2-C4) also exhibited p65 nuclear localization similar to that of C1 cells (data not shown). Second, the increased level of Bcl-2 protein was seen only in cells overexpressing *UEV1A* (Fig. 2(E)). Third, overexpression of *UEV1A* in HeLa cells also resulted in a 10-fold increase in NF-κB activity (data not shown). Finally, to critically examine whether the observed NF-κB activation in C1 cells is due to *UEV1A* overexpression, we selectively inhibited *UEV1* expression in C1 cells and found that reduced expression of Uev1A-Myc was accompanied by significant reduction of the number of cells with nuclear p65: from 43% to 10% (Fig. 2(C) and (D)). It should be noted that the remaining 10% of p65-positive cells have apparently reduced p65 intensity in the nucleus, probably due to reduced *UEV1A* expression. These observations collectively suggest that *UEV1A* plays a regulatory role in NF-κB activation.

UEV1 is required for TNFα-induced NF-κB activation

Numerous extracellular signals such as TNF, interleukins, UV irradiation, and bacterial or viral infections are able to induce NF-κB activity, which is required for immunity and inflammation response. In order to assess whether these stimuli also require the *UEV1* function, we treated control and C1 cells with 40 ng/mL TNFα or IL-1β for 2 hr and measured the NF-κB activity. As expected [45], the above treatments resulted in over 100-fold increase in NF-κB activity in control cells. Despite the 10-fold higher basal level of NF-κB activity in C1 cells, TNFα or IL-1β treatment of C1 cells did not induce the NF-κB activity higher than in control cells (Fig. 2(A)), indicating that these agents and *UEV1* act in the same pathway for NF-κB activation. To further ask if *UEV1* is required for TNFα induced NF-κB activation, we measured p65 immunostaining of TNFα treated cells. As seen in Figs. 2(C) and (D), TNFα treatment stimulated p65 nuclear localization in both control and C1 cells, and inhibition of *UEV1A* expression in C1 cells reduced TNFα induced nuclear translocation of p65 from 100% to 35%. The intensity of p65 nuclear staining in the remaining 35% of cells is apparently lower than that in corresponding cells without RNAi treatment (Fig. 2(C)), probably due to incomplete inhibition of *UEV1* expression in that subset of cells. Hence, we conclude that Uev1 is required for TNFα induced NF-κB activation, and possibly for induction by other stimuli as well.

UEV1A overexpression protects cells from stress-induced apoptosis

Since our results showed a significant up-regulation of Bcl-2 protein in C1 cells (Fig. 2(E)) and as NF-κB activation is considered to be a pro-survival and anti-apoptotic

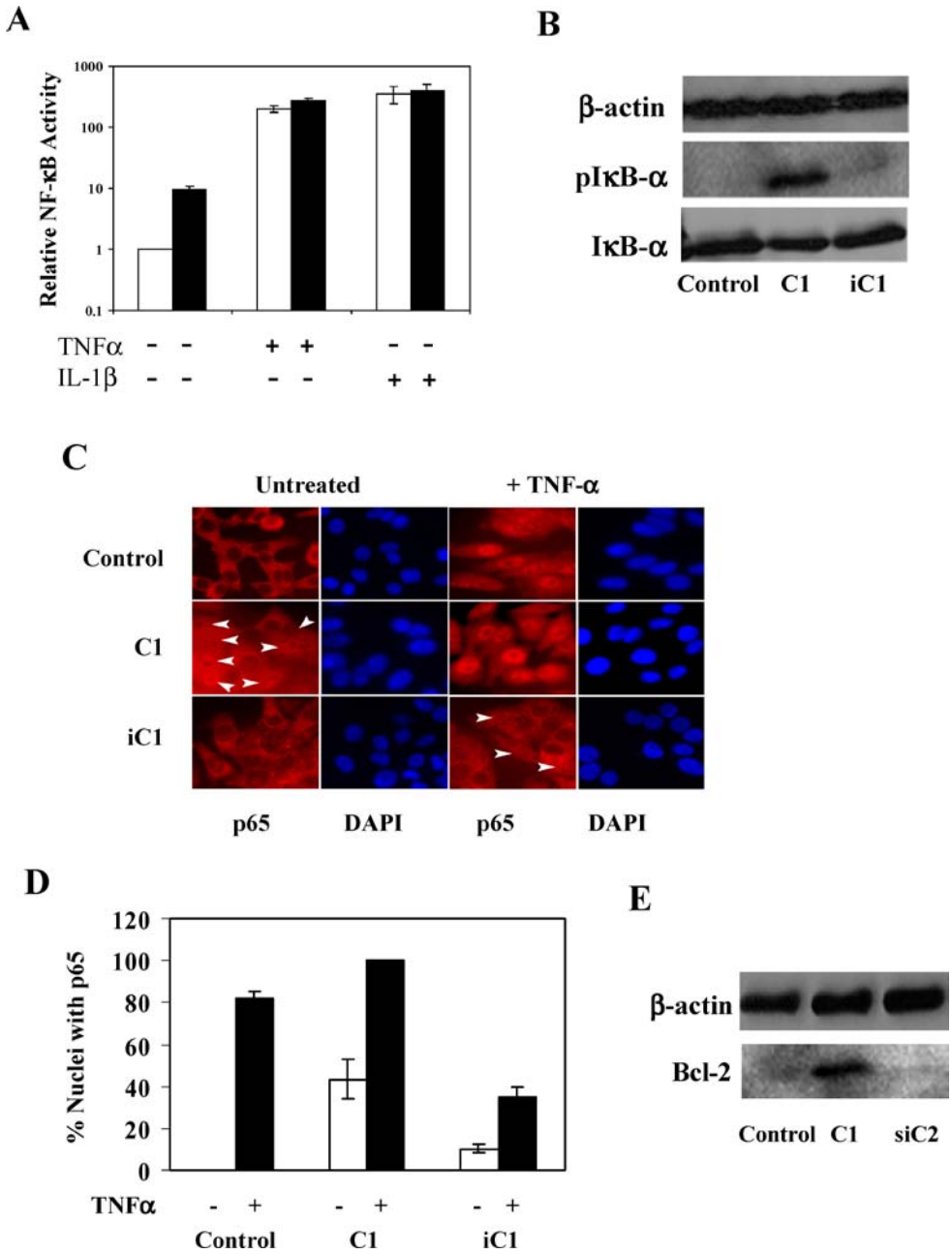

Fig. 2 NF-κB activity is increased by Uev1A overexpression. (A) NF-κB activity was measured in control and C1 cells either untreated or treated with 40 ng/mL TNFα or IL-1β for 2 hr as described in Materials and Methods and normalized to Renilla-transfected control activity. The results are an average of three independent experiments $\pm$SD. (B) Western blot analysis to detect phosphorylated (Ser32) (pIκBα) and total IκBα. Equal loading was monitored by β-actin detection. (C) Representative images of control (empty vector pcDNA), C1 and RNAi against *UEV1A*-transfected C1 cells (iC1) grown on glass cover slips either untreated or treated with TNFα and immunostained with an anti-p65 antibody as described in Materials and Methods. Left two panels represent untreated cells and right two panels represent TNFα treated (40 ng/mL for 2 hr) cells. Red images represent p65 immunofloures-cence and blue images are DAPI-stained nuclei of the same field. With images containing both p65-positive and p65-negative nuclei, arrows point to cells counted as p65-positive nuclei. Please note different intensity of p65-positive nuclear staining between C1 and iC1 cells after TNFα treatment. (D) Graphical summary of the results of p65 immunoflourescence on untreated or TNFα-treated control, C1 and iC1 cells. Results are an average of four independent experiments $\pm$SD. (E) Western blot analysis of Bcl-2 protein in control, C1 and siC1 cells. Equal loading was monitored by β-actin detection

response to environmental stresses, which has been linked to tumorigenesis, we asked whether overexpression of *UEV1A* also leads to protection of cells against stress-induced apoptosis. Apoptosis was assessed by flow cytometric and TUNEL assays on stable HepG2 cells exposed to two different apoptosis inducers, camptothecin (CPT) and staurosporine (STS). CPT is a DNA topoisomerase I inhibitor and is used as an anticancer chemotherapeutic agent [46, 47].

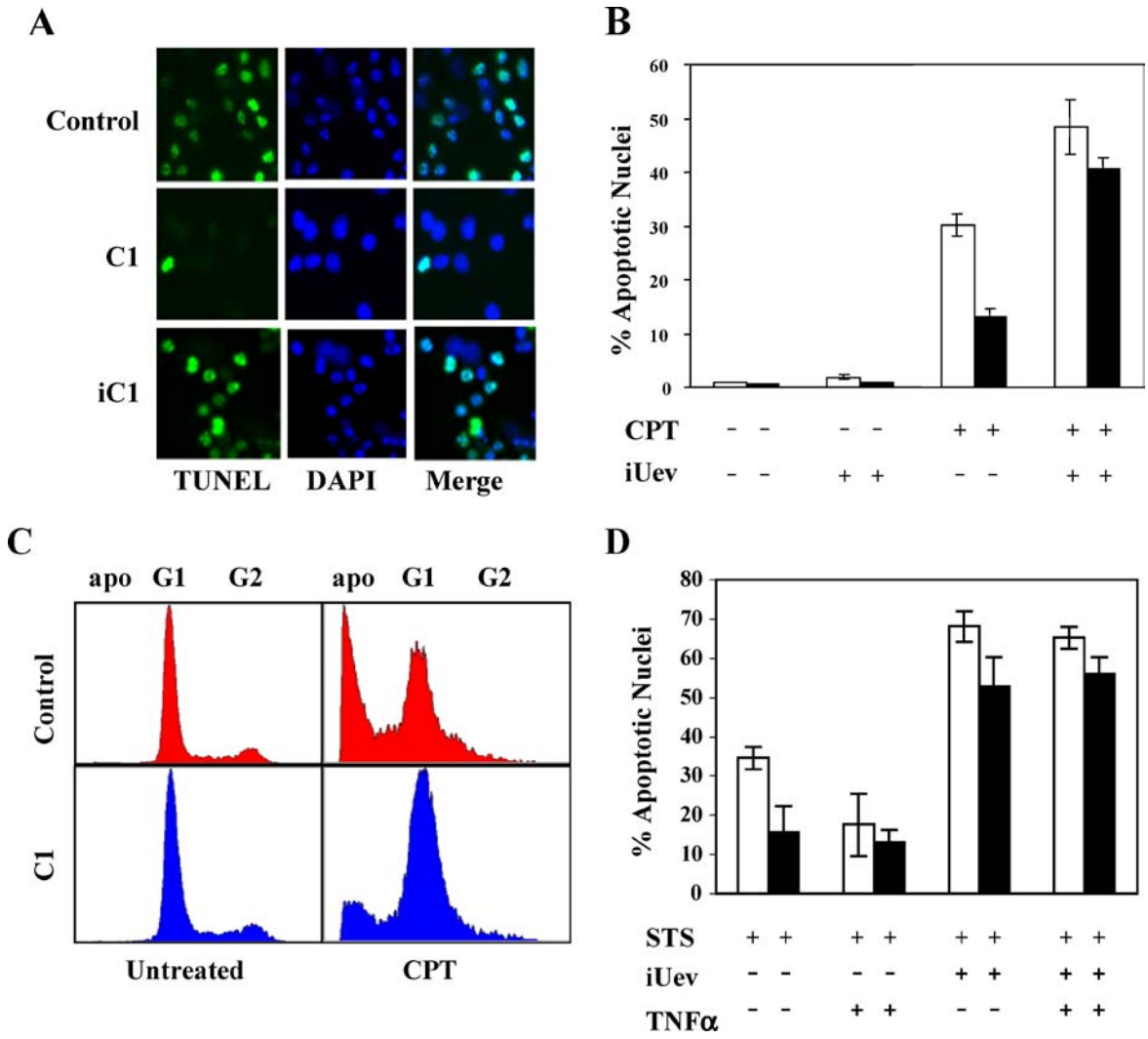

Fig. 3 *UEV1A* overexpression protects cells from stress-induced apoptosis. (A) Representative images of TUNEL apoptotic nuclei in CPT-treated (0.1 μM for 48 hr) control (top row) and C1 (middle row) and iC1 (bottom row) cells as described in Materials and Methods. The left panel (green) is the TUNEL data, middle panel is the corresponding DAPI nuclear staining and the right panel shows the merge of the previous two images illustrating apoptotic nuclei. (B) Graphical representation of TUNEL nuclei counted in control (open bars) and C1 (filled bars) cells with or without CPT and RNAi treatments against *UEV1* (iUev) as indicated. (C) Flow cytometry analysis was performed as described in Materials and Methods and % of apoptotic nuclei was determined in untreated (left panel) and CPT-treated (right panel) in control (top panel) and C1 (bottom panel) cells. (D) STS (1 μM for 24 hr) treated cells with or without TNFα (40 ng/mL) and RNAi treatments against *UEV1* (iUev) as indicated in graph. Open bars represent control and filled bars are C1 cells. The graphs represent the results of three independent experiments $\pm$SD. Untreated cells from all cell lines displayed about 1% apoptotic nuclei as judged by both assays

STS, a microbial alkaloid, is a potent broad-spectrum serine/threonine kinase inhibitor and is known to cause apoptosis in cultured cells [48, 49]. High-level (C1, Fig. 3) and low-level (C6, data not shown) expression of *UEV1A* in HepG2 cells conferred different degrees of protection against apoptosis triggered by both of these agents. Both TUNEL (Figs. 3(A) and (B)) and flow cytometric (Fig. 3(C)) analyses show that under conditions of 0.1 μM CPT treatment for 48 hrs, 13% of C1 cells undergo apoptosis compared to 30% apoptosis in control cells, whereas under the same experimental conditions, both untreated cells had only approximately 1% apoptotic nuclei. Inhibition of *UEV1* expression in C1 by RNAi resulted in an increase in TUNEL-positive nuclei to 40% with CPT treatment. Similar anti-apoptotic effects were also observed in parallel studies conducted with stable HeLa cells overexpressing Uev1A-Myc (data not shown). Correspondingly, C1 cells treated with 1.0 μM STS for 24 hr had lower number of apoptotic nuclei as compared to control and this protective effect was abolished when C1 cells were transfected with RNAi (Fig. 3(D)). Furthermore, TNFα activated NF-κB (Fig. 2) and conferred resistance to STS induced apoptosis in control and C1 cells (Fig. 3(D)). When these cells were subjected to RNAi against *UEV1* expression, the effect of TNFα was completely reversed (Fig. 3(D)).

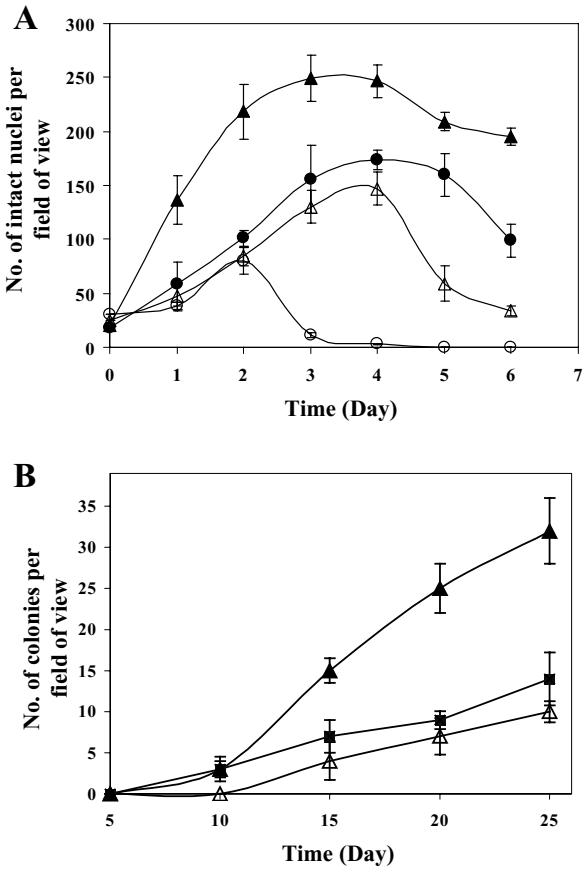

Fig. 4 *UEV1A* overexpression promotes cell growth in free serum media and on soft agar. (A) Growth curve of control and C1 cells under serum-supplemented and serum-deprived conditions. At least four different fields of view for each treatment were captured for statistical analysis, with standard deviations represented by error bars. (●) control cells with serum; (○) control cells without serum; (▲) C1 cells with serum; and (△) C1 cells without serum. (B) Graphical representation of soft agar assay of (■) control, (▲) C1, and (△) iC1 cells. At least three different fields of view for each day were taken for three independent experiments ± SD

Hence, our data demonstrates that *UEV1A* overexpression alone is sufficient to provide cells with protection against apoptosis induced by diverse environmental stresses and this effect is via the NF-κB signaling pathway.

UEV1A overexpression prolongs cell life in serum-free media and soft agar

It has been shown that many cultured cells undergo apoptosis when grown in serum-free culture medium [50] and tumor cells develop tolerance to nutrient deprivation [51]. We found that with serum deprivation, there was high viability of Uev1A-Myc overexpressing cells as compared to control (Fig. 4(A)), whereas the growth curve of low Uev1A-Myc expressing cells (C6) was not significantly different than that of control cells. With serum withdrawal, all cell lines initially showed similar growth; however, at day three control cells had only a 7% survival rate whereas C1 had over 50% viability and maintained linear growth for two more days. Under serum-supplemented conditions, initially, the C1 cell line had a higher growth rate than control. Afterwards, C1 had 40% more viable cells at day 3 and 30% more at day 4 compared to control. It is worth noting that serum-starved C1 cells had a similar growth pattern to serum-supplemented control cells for up to four days, but the growth rate significantly dropped after this time (Fig. 4(A)). Transfection of C1 cells with RNAi against *UEV1* decreased the survival duration of both serum-deprived and supplemented cells to the control levels. These experiments were confirmed with C2 (high Uev1A expression) and C6 (low Uev1A expression). Putting together, the growth factor-independent proliferation of C1 and C2 cells again substantiates our hypothesis that *UEV1A* promotes anti-apoptotic activity in cultured human cells and may aid in tumor progression [51].

In order to determine whether *UEV1A* overexpression promotes anchorage-independent cell growth, we assessed colony formation in soft agar. The colony growth was monitored by light microscopy of control transfected, C1 and C1 cells treated with RNAi against *UEV1* expression (iC1). As shown in Fig. 4(B), by day 10, the level of colony formation was indistinguishable between control and C1 cells. Thereafter, the control cell growth on soft agar tapered off, while C1 cells continued to form distinct colonies past day 25. Inhibition of *UEV1* expression in C1 cells completely abolished their growth advantage in soft agar. As a matter of fact, iC1 cells did not form a single colony by day 10. The subsequent colony formation in iC1 cells was probably due to the reduced inhibition of *UEV1* expression in subset of C1 cells over time. Nevertheless, the above observations that *UEV1A* overexpression enhanced survival capabilities under serum-deprived conditions and in soft agar as compared to control allow us to conclude that increased Uev1A alone is sufficient to promote cell survival and growth under restricted conditions, a hallmark of tumor cells.

Discussion

The activation of the NF-κB signal transduction pathway requires many proteins to be covalently modified and regulated by phosphorylation, sumoylation and ubiquitination for degradation [52–54]. Recently, the importance of Ubc13-Uev mediated Lys63-linked poly-Ub modifications of key participants in this pathway, such as NEMO, RIP1 and TRAFs has been demonstrated [18–20, 23, 25]. Constitutive activation of NF-κB is frequently observed in many cancer cells [21, 26]. It is very well established that abnormal NF-κB activation is also a hallmark of inflammatory response and cancer [34]. Activated NF-κB DNA binding complexes are known to elicit the expression of many genes,

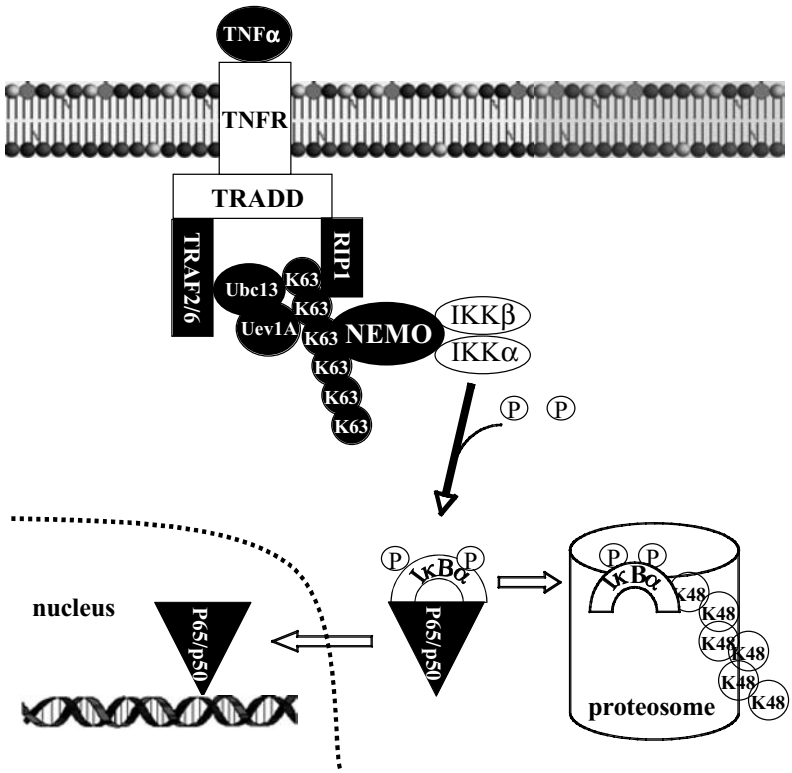

Fig. 5 Uev1A plays a key role in the NF-κB signaling pathway. A model depicting the involvement of the Ubc13-Uev1A heterodimer in the activation of NF-κB. Binding of TNFα to its receptor (TNFR) initiates the interaction between TRADD, RIP1 and TRAF2/6. Ubc13-Uev1A acts as an E2 to ubiquitinate NEMO and RIP1 via Lys63 chains, which is required for IκBα phosphorylation and NF-κB (p65 + p50) activation. Components important in this study are shown in solid boxes

including those required for anti-apoptotic pathways leading to prolonged cell survival and those for promotion of cell division. Among the anti-apoptotic proteins induced by NF-κB is Bcl-2, which is overexpressed in colon cancers [29, 30, 40, 41]. Several recent studies collectively suggest that inflammation and cancer are intimately connected. Indeed, this is the focus of emerging new research where studies have shown that chronic inflammation leads to tumor progression [31–34]. Specifically, Pikarsky et al. [32] have demonstrated that inflammation-associated NF-κB activation can give rise to sporadic liver cancer; additionally, chronic inflammation in ulcerative colitis has been linked to intestinal neoplasia and colorectal cancer [33, 55].

Our present study provides clear evidence that Uev1A plays a pivotal role in the NF-κB signal transduction pathway. We have experimentally achieved low-level constitutive activation of NF-κB in human cells by stably expressing high levels of *UEV1A* and demonstrated that *UEV1A* overexpression alone is sufficient to elicit NF-κB activation and inhibit apoptosis induced by diverse stress signals such as CPT, STS and serum starvation. The anti-apoptotic phenotype of Uev1A overexpressed cells could be partly due to the result of induced expression of Bcl-2 by the persistent activation of NF-κB in these cells. We suggest that the elevation of basal-level NF-κB activity upon stable overexpression of *UEV1A* can mimic the phenomena of chronic inflammation and that this observation is consistent with previous reports [1–3, 5] pointing to *UEV1* as a candidate proto-oncogene. Down-regulation of *UEV1* with RNAi reversed NF-κB activation in the *UEV1A* overexpression cell lines; this down-regulation was accompanied by elevated apoptosis upon stresses. *UEV1A* overexpression did not substantially further increase TNFα induced NF-κB activity over control cells, and furthermore abrogation of Uev1A by RNAi rendered cells susceptible to STS induced apoptosis which could not be reversed by TNFα. This indicates that Uev1A exerts its effects through the same pathway as TNFα. This observation appears to be highly relevant to tumorigenesis. For example, in inflammation-associated hepatocellular carcinoma, it was reported [32] that the inflammatory process triggers hepatocyte NF-κB through upregulation and release of TNFα from adjacent endothelial and inflammatory cells. We propose that this cellular condition can be created through overexpression of *UEV1A* as demonstrated through this study as well as observed with other tumor cell lines [5].

In this study we have provided strong evidence through several means that *UEV1A* can be categorized as a candidate proto-oncogene and therefore, we wish to further explore its functions in aiding tumorigenesis. Based on our present results and other recent reports, we would like to present a model (Fig. 5) emphasizing the role(s) of Ubc13-Uev1A in the complicated NF-κB signal transduction pathway. We hypothesize that the Ubc13-Uev1A heterodimer participates downstream of the TNF receptors (and probably IL-1/Toll-like receptors) along with TRAF proteins to ubiquitinate NEMO/IKKγ and RIP1 to activate IKK. Activated IKK leads

to the phosphorylation and degradation of IκBα, resulting in the activation of NF-κB. In cases where *UEV1A* is constitutively overexpressed beyond a certain threshold level, elevated basal NF-κB activity occurs and hence chronic inflammatory responses are instigated. Thus, Uev1A may serve as an important regulatory component for the activation of NF-κB; its abnormal up-regulation may be linked to a wide variety of cancers. Meanwhile, Uev1A may prove to be an important target for chemotherapy to reverse progression of tumorigenesis and to treat chronic inflammation-associated cancers.

Conclusion

Polyubiquitin chains attached to proteins via Lys63 modulate the function of target proteins. The Ubc13-Uev1A heterodimer has been shown to polyubiquitinate NEMO, a regulatory subunit of IKK, and RIP1, another activator in the NF-κB signaling pathway. Our results in HepG2 cells show that overexpressing Uev1A in this cell line is sufficient to cause NF-κB activation and Bcl-2 expression. As a result, HepG2 cells overexpressing Uev1A are able to grow in serum-deprived conditions and resist stress-induced apoptosis. Further studies will elucidate the precise mechanisms by which Uev1A is able to confer these characteristics on human cells. Our study implicates *UEV1A* as a potential proto-oncogene.

Acknowledgments We would like to thank Dr. V.M. Dixit for NF-κB luciferase reporter plasmids, Nida Syed for technical assistance and Michelle Hanna for proofreading the manuscript. This work was supported by The Cancer Research Society Inc. research grant to WX and NAS. NAS is supported by the Saskatchewan Health Research Foundation Postdoctoral Fellowship and PLA is supported by the University of Saskatchewan Graduate Teaching Fellowship.

References

1. Rothofsky ML, Lin SL (1997) *CROC-1* encodes a protein which mediates transcriptional activation of the human FOS promoter. Gene 195:141–149
2. Sancho E, Vila MR, Sanchez-Pulido L et al (1998) Role of UEV-1, an inactive variant of the E2 ubiquitin-conjugating enzymes, in *in vitro* differentiation and cell cycle behavior of HT-29-M6 intestinal mucosecretory cells. Mol Cell Biol 18:576–589
3. Ma L, Broomfield S, Lavery C et al (1998) Up-regulation of *CIR1*/*CROC1* expression upon cell immortalization and in tumor-derived human cell lines. Oncogene 17:1321–1326
4. Broomfield S, Chow BL, Xiao W (1998) *MMS2*, encoding a ubiquitin-conjugating-enzyme-like protein, is a member of the yeast error-free postreplication repair pathway. Proc Natl Acad Sci USA 95:5678–5683
5. Xiao W, Lin SL, Broomfield S, Chow BL, Wei YF (1998) The products of the yeast *MMS2* and two human homologs (*hMMS2 and CROC-1*) define a structurally and functionally conserved Ubc-like protein family. Nucleic Acids Res 26:3908–3914
6. Kallioniemi A, Kallioniemi OP, Piper J et al (1994) Detection and mapping of amplified DNA sequences in breast cancer by comparative genomic hybridization. Proc Natl Acad Sci USA 91:2156–2160
7. Tanner MM, Tirkkonen M, Kallioniemi A et al (1994) Increased copy number at 20q13 in breast cancer: defining the critical region and exclusion of candidate genes. Cancer Res 54:4257–4260
8. Tanner MM, Tirkkonen M, Kallioniemi A et al (1995) Amplification of chromosomal region 20q13 in invasive breast cancer: prognostic implications. Clin Cancer Res 1:1455–1461
9. Brinkmann U, Gallo M, Polymeropoulos MH, Pastan I (1996) The human *CAS* (cellular apoptosis susceptibility) gene mapping on chromosome 20q13 is amplified in BT474 breast cancer cells and part of aberrant chromosomes in breast and colon cancer cell lines. Genome Res 6:187–194
10. El-Rifai W, Harper JC, Cummings OW et al (1998) Consistent genetic alterations in xenografts of proximal stomach and gastro-esophageal junction adenocarcinomas. Cancer Res 58:34–37
11. Savelieva E, Belair CD, Newton MA et al (1997) 20q gain associates with immortalization: 20q13.2 amplification correlates with genome instability in human papillomavirus 16 E7 transformed human uroepithelial cells. Oncogene 14:551–560
12. Yeager TR, DeVries S, Jarrard DF et al (1998) Overcoming cellular senescence in human cancer pathogenesis. Genes Dev 12:163–174
13. McKenna S, Spyracopoulos L, Moraes T et al (2001) Noncovalent interaction between ubiquitin and the human DNA repair protein Mms2 is required for Ubc13-mediated polyubiquitination. J Biol Chem 276:40120–40126
14. McKenna S, Moraes T, Pastushok L et al (2003) An NMR-based model of the ubiquitin-bound human ubiquitin conjugation complex Mms2.Ubc13. The structural basis for lysine 63 chain catalysis. J Biol Chem 278:13151–13158
15. Moraes TF, Edwards RA, McKenna S et al (2001) Crystal structure of the human ubiquitin conjugating enzyme complex, hMms2-hUbc13. Nat Struct Biol 8:669–673
16. Hofmann RM, Pickart CM (1999) Noncanonical *MMS2*-encoded ubiquitin-conjugating enzyme functions in assembly of novel polyubiquitin chains for DNA repair. Cell 96:645–653
17. Pickart CM (2001) Mechanisms underlying ubiquitination. Annu Rev Biochem 70:503–533
18. Deng L, Wang C, Spencer E et al (2000) Activation of the IκB kinase complex by TRAF6 requires a dimeric ubiquitin-conjugating enzyme complex and a unique polyubiquitin chain. Cell 103:351–361
19. Wang C, Deng L, Hong M et al (2001) TAK1 is a ubiquitin-dependent kinase of MKK and IKK. Nature 412:346–351
20. Shi CS, Kehrl JH (2003) Tumor necrosis factor (TNF)-induced germinal center kinase-related (GCKR) and stress-activated protein kinase (SAPK) activation depends upon the E2/E3 complex Ubc13-Uev1A/TNF receptor-associated factor 2 (TRAF2). J Biol Chem 278:15429–15434
21. Lin A, Karin M (2003) NF-κB in cancer: a marked target. Semin Cancer Biol 13:107–114
22. Hayden MS, Ghosh S (2004) Signaling to NF-κB. Genes Dev 18:2195–2224
23. Zhou H, Wertz I, O'Rourke K et al (2004) Bcl10 activates the NF-κB pathway through ubiquitination of NEMO. Nature 427:167–171
24. Sun L, Deng L, Ea CK, Xia ZP, Chen ZJ (2004) The TRAF6 ubiquitin ligase and TAK1 kinase mediate IKK activation by BCL10 and MALT1 in T lymphocytes. Mol Cell 14:289–301
25. Ea CK, Deng L, Xia ZP, Pineda G, Chen ZJ (2006) Activation of IKK by TNFα requires site-specific ubiquitination of RIP1 and polyubiquitin binding by NEMO. Mol Cell 22:245–257

26. Debatin KM (2004) Apoptosis pathways in cancer and cancer therapy. Cancer Immunol Immunother 53:153–159
27. Azoitei N, Wirth T, Baumann B (2005) Activation of the IκB kinase complex is sufficient for neuronal differentiation of PC12 cells. J Neurochem 93:1487–1501
28. Chen GG, Liang NC, Lee JF et al (2004) Over-expression of Bcl-2 against *Pteris semipinnata* L-induced apoptosis of human colon cancer cells via a NF-κB-related pathway. Apoptosis 9:619–627
29. Chen GG, Lee JF, Wang SH et al (2002) Apoptosis induced by activation of peroxisome-proliferator activated receptor-gamma is associated with Bcl-2 and NF-κB in human colon cancer. Life Sci 70:2631–2646
30. O'Connell J, Bennett MW, Nally K et al (2000) Altered mechanisms of apoptosis in colon cancer: Fas resistance and counterattack in the tumor-immune conflict. Ann N Y Acad Sci 910:178–192
31. Ditsworth D, Zong WX (2004) NF-κB: Key mediator of inflammation-associated cancer. Cancer Biol Ther 3:1214–1216
32. Pikarsky E, Porat RM, Stein I et al (2004) NF-κB functions as a tumour promoter in inflammation-associated cancer. Nature 431:461–466
33. Clevers H (2004) At the crossroads of inflammation and cancer. Cell 118:671–674
34. Karin M (2005) Inflammation and cancer: the long reach of Ras. Nat Med 11:20–21
35. Yu JY, DeRuiter SL, Turner DL (2002) RNA interference by expression of short-interfering RNAs and hairpin RNAs in mammalian cells. Proc Natl Acad Sci USA 99:6047–6052
36. Andersen PL, Zhou H, Pastushok L et al (2005) Distinct regulation of Ubc13 functions by the two ubiquitin-conjugating enzyme variants Mms2 and Uev1A. J Cell Biol 170:745–755
37. Warrington RC, Norum JN, Hilchey JL, Watt C, Fang WD (2003) A simple, informative, and quantitative flow cytometric method for assessing apoptosis in cultured cells. Prog Neuropsychopharmacol Biol Psychiatry 27:231–243
38. Ke N, Albers A, Claassen G et al (2004) One-week 96-well soft agar growth assay for cancer target validation. Biotechniques 36:826–828, 830
39. Li Z, Xiao W, McCormick JJ, Maher VM (2002) Identification of a protein essential for a major pathway used by human cells to avoid UV- induced DNA damage. Proc Natl Acad Sci USA 99:4459–4464
40. Tamatani M, Che YH, Matsuzaki H et al (1999) Tumor necrosis factor induces Bcl-2 and Bcl-x expression through NF-κB activation in primary hippocampal neurons. J Biol Chem 274:8531–8538
41. Tamatani M, Mitsuda N, Matsuzaki H et al (2000) A pathway of neuronal apoptosis induced by hypoxia/reoxygenation: roles of nuclear factor-κB and Bcl-2. J Neurochem 75:683–693
42. Takehara T, Liu X, Fujimoto J, Friedman SL, Takahashi H (2001) Expression and role of Bcl-xL in human hepatocellular carcinomas. Hepatology 34:55–61
43. Emanuele S, Calvaruso G, Lauricella M et al (2002) Apoptosis induced in hepatoblastoma HepG2 cells by the proteasome inhibitor MG132 is associated with hydrogen peroxide production, expression of Bcl-XS and activation of caspase-3. Int J Oncol 21:857–865
44. Giuliano M, Bellavia G, Lauricella M et al (2004) Staurosporine-induced apoptosis in Chang liver cells is associated with down-regulation of Bcl-2 and Bcl-XL. Int J Mol Med 13:565–571
45. Chiao PJ, Na R, Niu J et al (2002) Role of Rel/NF-κB transcription factors in apoptosis of human hepatocellular carcinoma cells. Cancer 95:1696–1705
46. Champoux JJ (2001) DNA topoisomerases: structure, function, and mechanism. Annu Rev Biochem 70:369–413
47. Pommier Y, Pourquier P, Fan Y, Strumberg D (1998) Mechanism of action of eukaryotic DNA topoisomerase I and drugs targeted to the enzyme. Biochim Biophys Acta 1400:83–105
48. Weil M, Jacobson MD, Coles HS et al (1996) Constitutive expression of the machinery for programmed cell death. J Cell Biol 133:1053–1059
49. Miyamoto Y, Takikawa Y, De Lin S, Sato S, Suzuki K (2004) Apoptotic hepatocellular carcinoma HepG2 cells accelerate blood coagulation. Hepatol Res 29:167–172
50. Raff MC (1992) Social controls on cell survival and cell death. Nature 356:397–400
51. Izuishi K, Kato K, Ogura T, Kinoshita T, Esumi H (2000) Remarkable tolerance of tumor cells to nutrient deprivation: possible new biochemical target for cancer therapy. Cancer Res 60:6201–6207
52. Karin M, Ben-Neriah Y (2000) Phosphorylation meets ubiquitination: the control of NF-κB activity. Annu Rev Immunol 18:621–663
53. Huang TT, Wuerzberger-Davis SM, Wu ZH, Miyamoto S (2003) Sequential modification of NEMO/IKKγ by SUMO-1 and ubiquitin mediates NF-κB activation by genotoxic stress. Cell 115:565–576
54. Kracklauer MP, Schmidt C (2003) At the crossroads of SUMO and NF-κB. Mol Cancer 2:39
55. Greten FR, Eckmann L, Greten TF et al (2004) IKKβ links inflammation and tumorigenesis in a mouse model of colitis-associated cancer. Cell 118:285–296